

CALCULATION OF INTERACTION OF A TURBULENT  
NEAR-WAKE BEHIND A STEP WITH A SUPERSONIC JET

A. N. Antonov

UDC 532.526.4:532.525.2.001.24

Existing computational methods [1-5] do not enable one to calculate complex flows behind steps, accounting for nonuniformity of the incident supersonic flow and the effect of compression and expansion waves arriving in the near-wake region. For example, computational methods based on the methods of [1] or [2] are used mainly in uniform supersonic flow ahead of the base edge and, for the most part, cannot be used to calculate flow in annular nozzles with irregular conditions. An exception is reference [6], which investigated flow in an annular nozzle behind a cylindrical center-body. The present paper suggests a method, based on references [7, 8] for calculating the base pressure behind two-dimensional and three-dimensional steps, washed by a supersonic jet.

§1. We consider an approximate flow scheme in the base region behind a step, which provides for typical interaction of a turbulent boundary layer with an external perfect flow (Fig. 1). Between sections 1 and 2 there is expansion of the flow, AS is the line of constant mass flow rate, and S is the critical point. The dashed line indicates the boundary-layer edge. Immediately behind the body, between sections 2 and 3, there is a constant-pressure separated region, so that flow interaction begins at some section 3. The interaction of the viscous layers with the outer ideal flow (jet) was calculated using boundary-layer equations. According to [7], the following system of equations can be written for the interaction region:

$$d\delta^*/dx = F_0(M, \delta^*, \theta^{**}, \beta), \quad d\theta^{**}/dx = F_1(M, \delta^*, \theta^{**}), \quad (1.1)$$

$$dM/dx = F_2(M, \delta^*, \theta^{**}),$$

$$\text{where } F_0 = \text{tg } \beta + D; \quad F_1 = \Gamma^2 \xi - F_2 \frac{\theta^{**}}{M} (H + 2) - \frac{e\theta^{**}}{r} \frac{dr}{dx};$$

$$F_2 = -\frac{A^* M \Lambda^2}{T^0 H \delta^{**}}; \quad F_3 = M \frac{p_1}{p_{01}} \frac{a_{01}}{a_1}; \quad F_3' = \frac{dF_3}{dM}; \quad A^* = A^*(M^*); \quad M^* = \frac{M_2 + M_3}{2};$$

$$D = \frac{\delta^*}{F_3} \left( \frac{1}{h^*} - 1 \right) F_2 F_3'; \quad \xi = \frac{A^*}{T^0} \left( \frac{I_1}{I_{01}} \right)^{0.5\vartheta}; \quad \theta^{**} = \delta^{**} \left( \frac{I_1}{I_{01}} \right)^{0.5} \frac{\rho_1}{\rho_{01}};$$

$$T^0 = 0.5 I_w / I_{01} + 0.22 \text{Pr}^{1/3} + (0.5 - 0.22 \text{Pr}^{1/3}) I_1 / I_{01};$$

$$\vartheta = (\kappa + 1) / (\kappa - 1);$$

$$h^* = \frac{H I_{01} / I_1 + 0.5 (\kappa - 1) M^2}{H / H^* + 0.5 (\kappa - 1) M^2 (H + 1)}; \quad (1.2)$$

$$h = H I_{01} / I_1 + (I_{01} / I_1 - 1). \quad (1.3)$$

Here  $M$  is the Mach number at the edge of the boundary layer and  $\beta$  is the angle between the velocity vector at the boundary-layer edge and the  $Ox$  axis. The first equation of (1.1) for the variation in displacement thickness was obtained from a relation in [2], which takes into account mixing of the ideal part of the flow

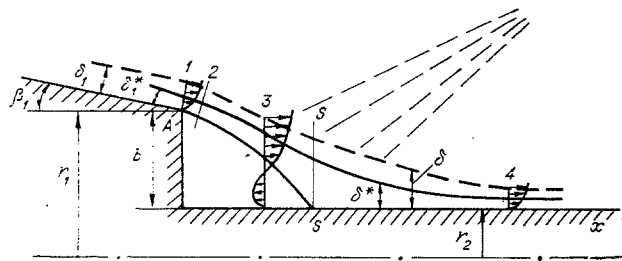


Fig. 1

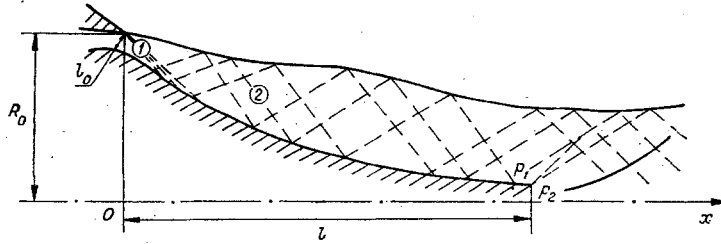


Fig. 2

into the boundary layer; the second equation is the momentum equation and the third connects the pressure-gradient parameter for a compressible boundary layer with the pressure-gradient parameter for the incompressible boundary layer. The ratios between the parameters of the incompressible turbulent layer  $H$ ,  $H^*$ ,  $\Gamma$ ,  $\Lambda$  appearing in Eq. (1.1) in the flow region between sections SS and 4 (attached boundary layer, see Fig. 1) were regarded as known and were chosen in the form of the relations  $H=H(\Lambda)$ ,  $\Gamma=\Gamma(H)$ ,  $H^*=H^*(H)$  given in [7].

The quantity  $\Lambda$  varies from  $\Lambda=0$  (zero-gradient flow) to  $\Lambda_S=0.1$  (the value of the pressure-gradient parameter  $\Lambda$  at the points of separation or reattachment of the boundary layer). For regions of separated gradient flow with reverse flow, i.e., in the flow region between sections 3 and SS (see Fig. 1), the quantities  $H$  and  $\Lambda$  are linked by the linear relation  $H=H_3+10(H_S-H_3)\Lambda$  ( $0\leq\Lambda\leq\Lambda_S$ ,  $H_3$  is the shape factor for the incompressible boundary layer in the initial section where the boundary layer interacts with the external perfect flow), and we can put approximately  $\Gamma=0$ . The dependence of  $A^*$  on  $M^*$ , obtained by correlating experimental results, was given in [7]. During the calculations, at each  $x$  step in integrating the system of equations (1.1), we determined the parameters  $M$ ,  $\delta^*$ ,  $\theta^{**}$  and found the momentum loss thickness  $\delta^{**}$ . Then the additional boundary-layer parameters  $h$ ,  $H$ ,  $\Lambda$ ,  $\Gamma$ ,  $H^*$ ,  $h^*$  were calculated, using Eqs. (1.1)-(1.3) and the relationships given graphically in [7].

In defining the base region flow we consider interaction of the boundary layer with the external perfect supersonic flow. For two-dimensional flow in equilibrium ahead of the base rim, we calculated the unbounded perfect flow using the Prandtl-Meyer relation, which relates the angle of turn of the velocity vector at the edge of the boundary layer with the Mach number variation:

$$\beta = v(M_1) - v(M) + \beta_1. \quad (1.4)$$

With this relation we can close the problem [we have the unknowns  $M$ ,  $\delta^*$ ,  $\theta^{**}$ ,  $\beta$  and the three differential equations in system (1.1) and Eq. (1.4)]. In the solution of the system of equations (1.1) in conjunction with Eq. (1.4), the boundary layer affects the perfect flow and the perfect flow affects the boundary layer. This kind of interaction of viscous and inviscid flows is typical of base region flow. For an axisymmetric flow, to calculate the external perfect flow, i.e., to obtain the parameter  $\beta$ , the method of characteristics is used (see [7, 8]); this method is also appropriate when the flow field ahead of the base rim is nonuniform and contains compression and rarefaction waves.

Knowing the parameters  $M$ ,  $\delta^*$ ,  $\theta^{**}$ ,  $\beta$  at the initial boundary-layer section 3, we can integrate the system (1.1) up to the end section 4. The initial conditions for system (1.1) describing the flow interaction in the near-wake behind the step, are determined from the condition that this flow should match the flow in the constant-pressure mixing zone [7]. We denote the boundary-layer thickness, the displacement thickness, the momentum loss thickness, the Mach number  $M$ , and the angle between the velocity vector at the edge of the boundary layer and the OX axis ahead of the step by the symbols  $\delta_1$ ,  $\delta_1^*$ ,  $\delta_1^{**}$ ,  $M_1$ ,  $\beta_1$ . Considering first two-dimensional flow, we shall assume that at section 2, where we have the value  $\beta_2 = v(M_1) - v(M_2) + \beta_1$ , the boundary layer starts up with parameters  $M_2$ ,  $\delta_2$ ,  $\delta_2^*$ ,  $\delta_2^{**}$ . We shall take the relations between the parameters  $\delta_1^{**}$  and  $\delta_2^{**}$  in the form [3]

$$\delta_2^{**}/\delta_1^{**} = f = (\rho_1 u_1 M_1^2)_1 / (\rho_1 u_1 M_1^2)_2.$$

We now determine the parameters in the constant-pressure zone. From the second equation of system (1.1) we calculate the displacement thickness  $\delta_2^*$ , and then, using the conditions for conservation of mass and conservation of momentum in the constant-pressure zone, we determine the momentum loss thickness  $\delta_2^{**}$ :

$$\delta_2^* = (\delta_1^* + b) + \varphi_- x, \quad \delta_2^{**} = \delta_1^{**}, \quad \varphi_- = \text{tg } \beta_2 \quad (M_- = M_2). \quad (1.5)$$

Matching of the interaction flow and the constant-pressure flow is accomplished through the condition that the displacement thickness and the momentum loss thickness are kept constant at section 3:

$$\delta_{3-}^* = \delta_{3+}^*, \quad \delta_{3-}^{**} = \delta_{3+}^{**}. \quad (1.6)$$

These two relations are sufficient to determine the parameters  $\delta_{3+}^*$  and  $\delta_{3+}^{**}$ , if the length of the constant-pressure region  $x_3$  is known. Calculating  $x_3$  using the method of [4], we obtain, from Eqs. (1.5) and (1.6),

$$\delta_{3+}^* = (\delta_1^* + b) + x_3 \operatorname{tg} \beta_2, \quad \delta_{3+}^{**} = f \delta_1^{**}, \quad M_{3+} = M_2. \quad (1.7)$$

These equations give us initial boundary conditions for integrating the system (1.1). For an axisymmetric flow the initial boundary conditions have the form

$$\delta_{3+}^* = (\delta_1^* + b) + \int_0^{x_3} \operatorname{tg} \beta dx, \quad \delta_{3+}^{**} = \frac{r_1}{r_2} f \delta_1^{**}, \quad M_{3+} = M_2. \quad (1.8)$$

For a uniform flow ahead of the base rim, the flow conditions on a flat plate or a cylindrical surface  $\beta_4 = 0$ ,  $\Lambda_4 = 0$ , serve as final boundary conditions at section 4. In solving the boundary problem for the system of differential equations (1.1) we integrate the system from section 3 to section 4 in the direction of the main flow; here a "ranging" method is used to choose a value of  $M_2$  (or  $p_2$ ) such that the parameters  $\beta_4 = 0$  and  $\Lambda_4 = 0$  are obtained at section 4.

As is shown experimentally [9], with a nonuniform flow ahead of the base rim, and also when there are no expansion waves, the flow in the near-wake has the same features as in uniform flow. However, in this case the end boundary conditions for the system (1.1) require supplementary information. We evaluate the parameter  $\beta_4$  at the end section of the interaction region (at section 4) for  $\Lambda_4 = 0$ . To do this we convert the compressible boundary-layer equations to incompressible boundary layer form and write equations for the zero-order and first-order moment of momentum at  $r_2 = \text{const}$  [4]:

$$\frac{d\theta^{**}}{dX} + \frac{\theta^{**}}{U_1} \frac{dU_1}{dX} (H + 2) = \Gamma^2; \quad (1.9)$$

$$\theta^{**} \frac{dH}{dX} = \frac{H(H+1)(H^2-1)}{2} \frac{\theta^{**}}{U_1} \frac{dU_1}{dX} + H(H^2-1)\Gamma^2 + (H+1)(H^2-1) \int_0^1 \Gamma_*^2 d(Y/\theta) \quad (1.10)$$

(here  $\Gamma_*^2 = \tau/\rho_1 U_1^2$ ).

By substituting the value  $\Lambda_4 = 0$  into Eqs. (1.9) and (1.10), and taking into account the first equation of system (1.1), we obtain

$$\operatorname{tg} \beta_4 = \Gamma^2 \frac{I_{01}}{I_1} \frac{A^*}{T^0} \left\{ \left( H - 1 - \frac{I_1}{I_{01}} \right) - (H + 1)(H^2 - 1) b_w \right\},$$

where  $b_w = \int_0^1 (\Gamma_* / \Gamma)^2 d(Y/\theta)$ ,  $0 < b_w < 1$ .

By giving experimental value to the base pressure and calculating  $\beta_1$  and  $\beta_4$  (for  $M_1 = 1.4-4$ ), we estimate the parameter  $\beta_4^0 = |\beta_4/\beta_1| \leq 0.03$ . The calculations show that the pressure distribution in the interaction region is practically independent of  $\beta_4^0$  if  $\beta_4^0 \leq 0.03$ . Therefore, for convenience we shall assume conditions of the following form for the final boundary conditions for a nonuniform flow ahead of the base rim:  $\beta_4 = 0$  and  $\Lambda_4 = 0$ . These boundary conditions coincide with the final boundary conditions with a uniform flow ahead of the step. In calculating the base pressure behind the step using the method suggested one must first determine the boundary-layer parameters before it separates,  $\delta_1$ ,  $\delta_1^*$ ,  $\delta_1^{**}$ . Then we choose the value of  $M_2$  in the constant-pressure region (zero-order approximation) and calculate the parameters  $\delta^*$ ,  $\delta^{**}$ , and  $\beta$  at the beginning of the interaction section 3, using Eqs. (1.7) or (1.8) for a two-dimensional or an axisymmetric flow, respectively. Thereafter we integrate the differential equations (1.1) up to the section where  $\Lambda = 0$ . This section is assumed to be behind the final section 4. If  $\beta_4 \neq 0$ , then a new value of  $M_2$  is adopted, and so on (the "ranging" process) until we obtain the value  $\beta_4 = 0$  with a given accuracy. The method allows us to calculate flow in the base region, both with a uniform and a nonuniform flow ahead of the base rim, and also where there are expansion and compression waves arriving in the near-wake region. This method was used when the base support radius  $r_2 \gg \delta_1$ . It is shown experimentally [4], that when the relative size of the base bracket  $r_2/r_1$  varies from zero to 0.3, the base pressure varies very little ( $\sim 5\%$ ). Therefore, for the case of no base bracket we can use this method and a relative size of  $r_2/r_1 \leq 0.3$ . Calculation of the base pressure behind the truncated central body of an annular nozzle was performed using the method suggested above and a base bracket size of  $r_2/r_1 = 0.3$ .

§2. We now examine the flow at the base region formed with a truncated central body in an annular nozzle. Currently available publications [10, 11] deal mainly with numerical and experimental investigations of the design conditions for annular nozzles with a full-length central body. Irregular operation conditions for an annular nozzle with a covered crank-type support and a full-length central body are considered in [12], where a detailed experimental and theoretical investigation was made into flows where the external pressure

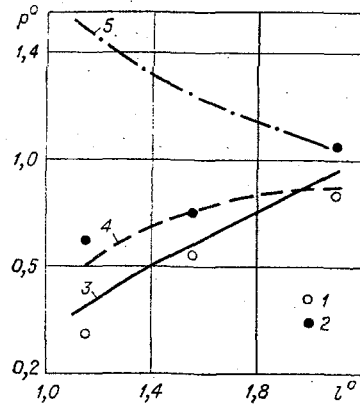


Fig. 3

$p_e$  is greater than the pressure  $p_a$  in the one-dimensional approximation from the ratio of the nozzle exit section area to the throat area. Using the method of characteristics, one can calculate the flow in an annular jet washing the central body. Here no density discontinuities arise in the jet and there are only compression and expansion shock waves. The condition for minimum total losses, allowing for friction, equivalent weight, and other factors reduces to the fact that in the actual conditions we are interested in practice in nozzles with a truncated central body. The end of such a body is acted on by the base pressure, which in the general case must improve the thrust characteristics of an annular nozzle.

Using the above method we calculated the base pressure behind a truncated central body for an annular nozzle with a covered crank, at Mach number  $M_a = 3.71$ . The pressure ratio factor  $n$  varied from 0.1 to 0.6 ( $n = p_a/p_e$ ,  $p_a = \pi(M_a)p_0$ ).

We can compare the computations with the results of experiments performed by Vilenskii [12] in air, where the characteristic dimensions of the annular nozzle were  $R_0 = 51$  mm and  $l_0/R_0 = 0.06$ , and the length of the truncated central body varied in the range  $1 < l^0 < 2.1$  ( $l^0 = l/R_0$ , and  $l$  is the length of the central body). Figure 2 shows a flow picture in the annular jet washing a truncated central body. The rarefaction waves 1, coming from the edge of the crank, are reflected from the surface of the central body and reach the jet boundary, from which compression waves 2 are reflected. Thus, there is a complex flow between the body and the jet boundary, containing both expansion waves and compression waves. This flow was calculated by the method of characteristics by Volkonskaya [12]. In order to calculate the base pressure behind the truncated central body of the annular nozzle (and also to calculate the flow in the jet after the flow turns behind the base rim), we first used the method of [12] for each value of  $l^0$  and  $n$ , to calculate the flow ahead of the nozzle rim; and from the pressure distribution on the central body, we used the method of [13] to find the characteristic boundary-layer thicknesses  $\delta_1^*$  and  $\delta_1^{**}$ . Then we calculated the flow in the base region, and in computing the outer perfect flow (an ideal supersonic jet) we used the flow parameters on a characteristic of the first family coming from a ray point on the base surface and reaching the jet boundary.

The results of the calculations of the base pressure  $p_0$  using this method for pressure ratio factors  $n = 0.148$  and  $n = 0.6$  are shown in Fig. 3 (theoretical curves 3 and 4), and the experimental results are shown

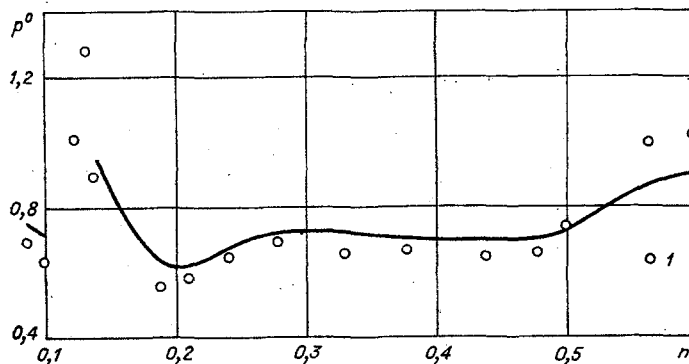


Fig. 4

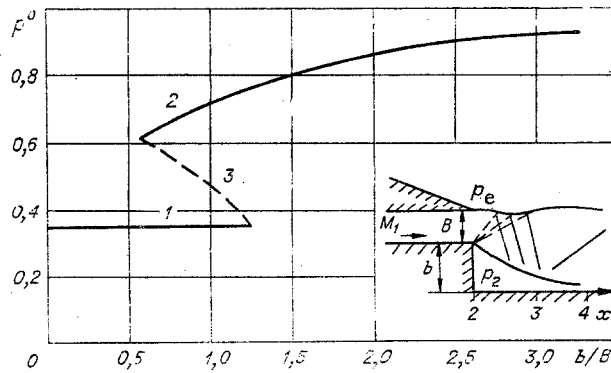


Fig. 5

by points 1 and 2 for  $n=0.148$  and  $0.6$ , respectively. It can be seen that the computations are in good agreement with the experimental results. We note that perturbations of the outer flow (in this case they are expansion waves) have an appreciable influence on the flow, reducing the base pressure. If we calculate for  $n=0.148$  without accounting for these perturbations (e.g., using the method of [14] and the equivalent surface and interpolation relations proposed there), the results (curve 5) are markedly different from the experimental data. It should be noted that for  $l^0=2.12$  and  $n=0.148$  a very weak expansion wave reaches the base region. Therefore, the calculated curves 3 and 5 obtained with this method and the method of [14] are in close agreement. For  $l^0=1.1$  and  $n=0.148$  a strong expansion wave reaches the base region, the Mach number on the first family characteristic coming from a ray point on the base varies from  $M_1=1.96$  on the surface of the central body to  $M_2=2.4$  on the jet boundary, while the angle between the velocity vector and the  $Ox$  axis varies from  $-14.5^\circ$  to  $0$ . This leads to an appreciable reduction of base pressure. The investigations which have been conducted (e.g., for  $n=0.6$  and  $l^0=1.5-2.1$ ) show that the compression wave reaching the base region increases the base pressure. As the strength of this wave increases the base pressure rises, and for some intensity of the wave there comes a time when  $p^0 > 1$ . In this case a compression shock leaves the edge of the base rim.

Since the computer program was not suitable for calculating flow with a compression shock, the calculation was carried out only for  $p^0 \leq 1$ . The points 1 on Fig. 4 show the base pressure as a function of the pressure ratio parameter  $n$  for  $l^0=2.1$  obtained experimentally. With variation in  $n$  the base pressure varies from  $0.56$  to  $1.27$ , and the maxima in  $p^0$  are seen to be at  $n \approx 0.13$  and  $0.6$ . For the range  $0.12 \leq n \leq 0.14$ , the base pressure becomes greater than  $1$ . Flow calculations made by means of the method of characteristics ahead of the base rim [12] for this range of  $n$  ( $0.12 \leq n \leq 0.14$ ) show that a strong compression wave reaches the base region. Figure 4 shows the results of our calculations (solid lines) for the region of values  $p^0 < 1$ . The calculations made show that the proposed method can be applied to determine the base pressure behind a truncated central body of an annular nozzle with a covered crank.

§3. In some structures one can meet the case where the base pressure behind a two-dimensional step, formed by structural elements, depends on the transverse size of the jet flowing above the step. We consider flow in the base region behind a two-dimensional step, washed by a supersonic jet with a pressure ratio factor  $n=p_1/p_e=1$  (Fig. 5). Perturbations arise at the edge of the step as expansion waves are propagated in the jet, reach the jet boundary, and, reflected as compression waves, arrive at the base region, affecting the flow there. There is complex interaction between the turbulent wake and the outer supersonic jet. By writing the boundary conditions at the jet boundary, i.e.,  $p_2=p_e=\text{const}$ , and using the above method, we can calculate the base pressure. The results of calculations for  $M_1=2$ ,  $\beta_1=0$ ,  $\delta_1^{**}/b=0.02$ , and  $n=1$  are shown in Fig. 5, where  $B$  is the jet width,  $b$  is the step height, and  $p_e$  is the pressure in the submerged space in which the jet is flowing. In contrast with the calculations made in Sec. 2 for an annular jet with  $n=0.1-0.6$  and  $l^0=1-2.2$ , and which yielded a unique solution to the problem, in the present case (for  $M_1=2$ ,  $n=1$ ,  $b/B=0.58-1.23$ ) we obtain three solutions. In the regions  $0 < b/B < 0.58$  and  $1.23 < b/B < 3.33$  a single solution is found. With increase in the parameter  $b/B$  from  $0$  to  $0.58$  the base pressure remains constant and a change in the jet width does not affect the flow in the base region. The reason is that the compression waves coming from the jet boundary do not strike the near-wake region (2-3-4). With a variation of  $b/B$  in the range  $1.25$  to  $3.33$  the base pressure increases, and a compression wave reaches the interaction region behind the step, causing an increase in base pressure. For  $0.58 < b/B < 1.25$  there are three solutions (see Fig. 5, curves 1-3). For the second solution no compression wave reaches the interaction region, and the length of the 2-3-4 region is less than the length of this region corresponding to the second solution. The third solution is an

intermediate case, where a compression wave from only a small part reaches the interaction zone in the neighborhood of Sec. 4.

Thus, in a nonuniform flow containing compression and expansion waves, the interaction of a turbulent wake with an outer supersonic stream (a supersonic jet) can have a more complex and nonunique character than the interaction of a turbulent wake with an outer supersonic uniform unbounded flow.

#### NOTATION

$x, y$ , longitudinal transverse coordinates;  $X, Y$ , transformed coordinates;  $\delta, \delta^*$ , and  $\delta^{**}$ , thickness, displacement thickness, and momentum thickness of the compressible boundary layer, respectively;  $\theta, \theta^*$ , and  $\theta^{**}$ , thickness, displacement thickness, and momentum thickness of the incompressible boundary layer, respectively;  $u, U$ , velocity in the compressible and incompressible boundary layers;  $\rho, \rho'$ , density of the compressible and incompressible boundary layers;  $\mu, \mu'$ , dynamic viscosity of the compressible and incompressible boundary layers;  $M$ , Mach number;  $p$ , pressure;  $a$ , sound speed;  $I$ , enthalpy;  $\tau$ , friction stress;  $Pr$ , Prandtl number;  $b$ , height of the step;  $r, r_1$ , and  $r_2$ , radius, radius of the base, and radius of the base bracket, respectively;  $\nu$ , Prandtl-Meyer angle;  $\varepsilon = 0$ , for two-dimensional flow;  $\varepsilon = 1$ , for axisymmetric flow. Indices: 0, stagnation flow; 1, at the outer edge of the boundary layer or ahead of the step; 2, at the outer edge of the mixing zone, immediately behind the step;  $w$ , parameters at the wall;  $+$ , in the interaction region;  $-$ , in the constant-pressure flow region;

$$h = \delta^*/\delta^{**}, h^* = \delta^*/\delta, h^{**} = \delta^{**}/\delta, H = \theta^*/\theta^{**}, H^* = \theta^*/\theta, \\ H^{**} = \theta^{**}/\theta, \kappa = c_p/c_v, \\ \tau_w = \gamma^2 \rho_1 u_1^2, \tau'_w = \gamma^2 \rho'_1 U_1^2, \lambda^2 = \left| \frac{\delta^*}{u_1} \frac{du_1}{dx} \right|, \Lambda^2 = \left| \frac{\theta^*}{U_1} \frac{dU_1}{dX} \right|, \\ v = \left( \frac{\kappa + 1}{\kappa - 1} \right)^{1/2} \arctg \left( \frac{\kappa - 1}{\kappa + 1} (M^2 - 1) \right)^{1/2} - \arctg \sqrt{M^2 - 1}, p^0 = p_2/p_1.$$

#### LITERATURE CITED

1. G. Korst, "Theory for the base pressure in transonic and supersonic flow," *Sb. Per. Mekh.*, No. 5 (45) (1957).
2. L. Crocco and L. Lees, "Mixing theory to determine the interaction of dissipative and near-isentropic flows," *Vopr. Raketn. Tekh.*, No. 2 (1953).
3. J. Nash, "An analysis of two-dimensional turbulent base flow, including the effect on the approaching boundary layer," *ARC RM*, N3344 (1963).
4. H. McDonald, "The turbulent supersonic base pressure problem: a comparison between a theory and some experimental evidence," *Aeronaut. Q.*, No. 17, 2 (1966).
5. J. E. Alber and L. Lees, "Integral theory for supersonic turbulent base flow," *AIAA J.*, 6, No. 7 (1968).
6. Sewell and Mueller, "The flow field and base pressure in nozzles with a central body," *Vopr. Raketn. Tekh.*, No. 2 (1974).
7. A. N. Antonov, "Calculation of the interaction of a turbulent boundary layer with the outer supersonic stream behind an obstacle," *Izv. Akad. Nauk SSSR, Mekh. Zhidk. Gaza*, No. 3 (1971).
8. A. N. Antonov, "Calculation of the interaction of a turbulent boundary layer with the outer supersonic flow in a concave corner and on the spherical aft section of a body," *Zh. Prikl. Mekh. Tekh. Fiz.*, No. 1 (1976).
9. A. F. Charwat, G. H. Burghart, and W. H. Nurick, "Base wakes in accelerates supersonic free streams," *Heat Transfer Fluid Mech. Inst.*, No. 2 (1967).
10. U. G. Pirumov and V. A. Rubtsova, "Design of axisymmetric supersonic annular nozzles," *Izv. Akad. Nauk SSSR, Mekh. Mashinostr.*, No. 6 (1961).
11. Migdal, Horgan, and Chamay, "An experimental evaluation of plug cluster nozzles," *AIAA J.*, No. 7 (1964).
12. F. A. Vilenskii, T. G. Volkonskaya, V. P. Gryaznov, and U. G. Pirumov, "Investigation of pressure ratio conditions in an axisymmetric annular nozzle with a center body," *Izv. Akad. Nauk SSSR, Mekh. Zhidk. Gaza*, No. 4 (1972).
13. V. S. Avdúevskii, B. M. Antonov, and N. A. Anfimov, *Basic Theory of Spacecraft Flight* [in Russian], *Mashinostroenie*, Moscow (1972).
14. M. Ya. Yudelovich, "An approximation method for calculating the base pressure for bodies of spherical shape," *Izv. Akad. Nauk SSSR, Mekh.*, No. 3 (1965).